

Supporting Information for

**Acid-Functionalized SBA-15-Type Periodic Mesoporous Organosilicas and their Use in the
Continuous Production of 5-Hydroxymethylfurfural**

Mark H. Tucker, Anthony J. Crisci, Bethany N. Wigington, Neelay Phadke, Ricardo Alamillo

Jinping Zhang, Susannah L. Scott, James A. Dumesic

Table of Contents	Page
Pre-catalysis characterization of E90, E45, and E0	S2
Fructose dehydration in a batch reactor	S3
Reactor design for extended operation	S4
Effect of linear velocity on initial rates	S4
Table S1 Results of fructose dehydration in a batch reactor	S7
Table S2 Dependence of fructose conversion on feed flow rate during extended catalyst operation	S8
Table S3 Initial rates and first-order deactivation rate constants at different space velocities	S10
Figure S1 Solid-state ^{13}C CP/MAS spectra of E90, E45, and E0	S10
Figure S2 Solid-state ^{29}Si MAS spectra of E90, E45, and E0	S11
Figure S3 N_2 adsorption/desorption isotherms of E90, E45, and E0	S12
Figure S4 X-ray diffraction patterns of E90, E45, and E0	S13
Figure S5 Alternative $\frac{1}{4}$ " reactor configuration	S14
Figure S6 Solid-state ^{29}Si MAS spectra of E90 and E45, before and after their use on-stream	S15

Pre-catalysis characterization of E90, E45, and E0. During the synthesis of each catalyst, MPTMS is efficiently oxidized *in situ* to the corresponding sulfonic acid by H₂O₂; no signal at 27 ppm (for $\equiv\text{SiCH}_2\text{CH}_2\text{CH}_2\text{SH}$) was observed in any of the ¹³C CP/MAS NMR spectra, Figure S1, ruling out the presence of unreacted thiopropyl groups. Three signals representing the anchored propylsulfonic acid groups are visible in each spectrum. The signal for the methylene bonded directly to Si appears at 11 ppm ($\equiv\text{SiCH}_2\text{CH}_2\text{CH}_2\text{SO}_3\text{H}$), and for the adjacent methylene ($\equiv\text{SiCH}_2\text{CH}_2\text{CH}_2\text{SO}_3\text{H}$) at 18 ppm. The methylene bonded to S produces a signal at 54 ppm.¹ A signal representing bridging ethane groups ($\equiv\text{SiCH}_2\text{CH}_2\text{Si}\equiv$) appears at 3 ppm,² Figures S1a,b. Although CP/MAS experiments are not strictly quantitative, the intensities of the signals due to the propylsulfonic acid groups relative to those of the bridging ethane groups are consistent with the composition of each material. The acid loading (mmol/g) decreases with increasing incorporation of BTME in the framework, since the latter has a higher molecular weight than TEOS.

All three ¹³C CP/MAS NMR spectra show additional signals at 70, 59, and 16 ppm. The peak centered at 70 ppm is associated with the residual templating surfactant that remains after solvent extraction. The intensity of this signal relative to the propylsulfonic acid group signals increases with BTME incorporation. Since it becomes more difficult to extract the template as the framework carbon content increases. The signals at 59 and 16 ppm represent adsorbed ethoxy groups resulting from the condensation of ethanol with surface silanols during template extraction.

The ²⁹Si NMR descriptor, T^{*n*} (where *n* is the number of SiOSi bonds), designates a silicon atom with one covalent bond to carbon and up to three siloxane bonds. In contrast, Q^{*n*} sites (where *n* is again the number of siloxane bonds) possess no Si-C bonds. They are produced in the

condensation of tetraalkoxysilanes to yield silica. As expected, T^2 and/or T^3 sites are observed in the ^{29}Si MAS NMR spectra of all the materials, while Q^3 ($(\text{SiO})_3\text{SiOR}$) and Q^4 ($(\text{SiO})_4\text{Si}$) sites are observed only in the spectra of E45 and E0, Figure S2. For E90 and E45, the T^2 and T^3 signals appear at -58 and -67 ppm, respectively, representing both BTME incorporated into the framework ($\text{SiCH}_2\text{CH}_2\text{Si}$) and the anchored acid sites ($\text{SiCH}_2\text{CH}_2\text{CH}_2\text{SO}_3\text{H}$), Figures S2a,b. In contrast, the T^3 site in the ^{29}Si MAS NMR spectrum of E0 represents only the anchored acid, Figure S2c. For this material, the T:Q ratio, or the ratio of functionalized silicon to bulk silicon, is close to the MPTMS:TEOS ratio used in the synthesis (1:10). For E45, the T:Q ratio (3:1) is also equal to the synthesis ratio, Figure S2b. Figure S2a shows that E90 contains only T sites, since a tetraalkoxysilane is not used in its synthesis.

Fructose dehydration in a batch reactor. Preliminary batch reactions were performed to determine the amount of each catalyst necessary to achieve high (> 80 %) fructose conversion in thick-walled glass reactors (10 mL, Alltech), Table S1. From this data, the catalyst masses were calculated for use in the $\frac{1}{4}$ " Simple Packed-Bed Reactor. In addition, the dehydration of fructose by unmodified silica gel (50 mg) was evaluated. The reactions were carried out in thick-walled glass reactors (10 mL, Alltech) using 1.5 g of a 2 wt% fructose solution dissolved in 4:1 (wt:wt) THF: Milli-Q water. A triangular magnetic stirring bar and one of E90, E45, E0 or $\text{pSO}_3\text{H-SC}$ (50 mg) were added to each reactor. The reactors were sealed using Teflon liners (Alltech) inserted into plastic caps and heated in a 16-well oil-filled aluminum block maintained at 403 K and stirred at 500 rpm. The temperature was maintained using a Fisher Scientific Isotemp digital stirring hotplate equipped with a temperature probe. After 100 min, each reactor was cooled in a slurry of dry ice and ethylene glycol. The reaction products were analyzed using the methods

described in the main text. The rate of HMF production was calculated by dividing the moles of HMF produced by the time and the catalyst mass.

Reactor design for extended operation. Extended operation with E90, E45, and E0 catalysts was studied using the 1/4" reactor configuration shown in Figure S5. The catalyst powder was mixed with 2 g crushed, fused SiO₂ chips (Sigma). In addition, a layer of silica chips was placed both above (0.36 g) and below (0.36 g) the catalyst bed. At the top and bottom of the reactor, quartz wool (Grace) was used to hold the bed in place. The reactor was well-insulated and heated to 403 K with a furnace. During the course of the reaction, the feed flow rate was adjusted (20-130 $\mu\text{L min}^{-1}$) to maintain appreciable conversions (65 – 25 %), Table S2. The times-on-stream in the flow reactor for E90, E45, and E0 were 148, 190, and 166 h, respectively. After each experiment, the reactor was cooled, then flushed with ca. 100 mL 4:1 (w:w) THF:Milli-Q water to remove physisorbed material. Each catalyst was dried in the reactor at 373 K under flowing He (Airgas). The catalysts were separated from the SiO₂ chips with a wire sieve for subsequent analysis by SEM and TEM.

Effect of linear velocity on initial rates. Using the reactor configuration shown in Figure 1a, the performance of catalyst 90E was tested using two different linear velocities, while keeping the weight hourly space velocity (WHSV) constant, Table S3. This led to an increase in the initial rate of HMF production. The Mears' criterion and Weisz-Prater number were estimated to verify that the reaction was not under external or internal diffusion limitations. The Mears' criterion is given by Equation S1:³

$$\frac{\Re R_p}{C_b k_c} < \frac{0.15}{n} \quad (\text{S1})$$

where \mathfrak{R} is the reaction rate (per unit volume of catalyst), R_p is the catalyst particle radius, C_b is the bulk phase reactant concentration, k_c is the mass transfer coefficient, and n is the reaction order. The reaction rate per unit catalyst volume, calculated by dividing the reaction rate ($23 \mu\text{mol min}^{-1} \text{g}^{-1}$) by the pore volume ($0.46 \text{ cm}^3 \text{ g}^{-1}$, Table 1), is $8.3 \times 10^{-7} \text{ mol s}^{-1} \text{ cm}^{-3}$. The particle radius, estimated using the SEM image in Figure 4a, is $0.5 \mu\text{m}$. The bulk concentration for the 2 wt% fructose solution in 4:1 THF:H₂O solution is $1.0 \times 10^{-4} \text{ mol cm}^{-3}$. To calculate the mass transfer coefficient, a dimensionless relationship applicable at low Reynolds numbers, eq S2, was used.⁴ It relates the Sherwood, Reynolds, and Schmidt numbers:

$$Sh_{part} = \frac{1.13}{\epsilon} Re_{part}^{1/3} Sc^{1/3} \quad (\text{S2})$$

where Sh_{part} and Re_{part} were calculated using the estimated particle diameter. A void fraction (ϵ) of 40 % was assumed. The diffusivity for fructose was approximated using the diffusivity for glucose in water, $7.0 \times 10^{-6} \text{ cm}^2 \text{ s}^{-1}$.⁵ The viscosity was approximated by extrapolating the viscosity of water to 130 °C, and the density was measured to be 0.92 g cm^{-3} . For 90E with 346 mg catalyst and a WHSV of 0.48 h^{-1} the Mears' criterion is 3.2×10^{-6} , indicating negligible external mass transfer limitations (limit: 0.15 n^{-1} , n = reaction order).

The Weisz-Prater number was calculated using eq S3:⁶

$$N_{W-P} = \frac{\mathfrak{R} R_p^2}{C_s D_{eff}} \quad (\text{S3})$$

where \mathfrak{R} and R_p are the reaction rate and particle radius (as defined for the Mears' criterion), C_s is the reactant concentration at the external surface of the particle, and D_{eff} is the effective diffusivity in the pores of the catalyst. Due to the low value of the Mears' criterion, the surface concentration can be assumed to be equal to the bulk concentration, $1.0 \times 10^{-4} \text{ mol cm}^{-3}$. The

effective diffusivity of fructose in the 4.2 nm pores was estimated, by extrapolation of literature data for glucose in water-filled pores,⁵ to be $3.35 \times 10^{-8} \text{ cm}^2 \text{ s}^{-1}$. The Weisz-Prater number was therefore calculated to be 6.1×10^{-4} , indicating that the reactions are free of internal mass transfer limitations (a Weisz-Prater number less than 0.3 indicates negligible internal mass transfer limitations).⁶

The low values for the Mears' criterion and Weisz-Prater number, mean that mass transfer limitations appear to be negligible. Consequently, we hypothesized that the dependence of the apparent rate constant on the amount of catalyst is the result of the liquid channeling through the fine powder catalyst. The reactor configuration was therefore changed to decrease the bed length, and the WHSV was increased. With these modifications, the rate became independent of linear velocity, indicating that liquid channeling in the reactor had been minimized.

References

- (1) Margolese, D.; Melero, J. A.; Christiansen, S. C.; Chmelka, B. F.; Stucky, G. D. *Chem. Mater.* **2000**, *12*, 2448.
- (2) Liu, J.; Yang, Q.; Kapoor, M. P.; Setoyama, N.; Inagaki, S.; Yang, J.; Zhang, L. *J. Phys. Chem. B* **2005**, *109*, 12250.
- (3) Dumesic, J. A.; Rudd, D. F.; Aparicio, L. M.; Rekoske, J. E.; Treviño, A. A. *The Microkinetics of Heterogeneous Catalysis*; American Chemical Society: Washington, D.C., 1993.
- (4) Seguin, D.; Montillet, A.; Brunjail, D.; Comiti, J. *Chem. Eng. J.* **1996**, *63*, 1.
- (5) Netrabukkana, R.; Lourvanij, K.; Rorrer, G. L. *Ind. Eng. Chem. Res.* **1996**, *35*, 458.
- (6) Vannice, M. A. *Kinetics of Catalytic Reactions*; Springer: New York, 2005.

Table S1. Results of fructose dehydration in a batch reactor^a

Catalyst	Reaction Time	Conversion	Selectivity
	min	%	%
pSO ₃ H-SC	70	91	67
E90	40	64	62
E45	40	68	68
E0	40	79	72

^a Reactions were conducted at 403 K with 1.5 g of a 2 wt % fructose in THF/water (4:1 wt:wt) and 50 mg catalyst.

Table S2. Dependence of fructose conversion on feed flow rate during extended catalyst operation

0E			45E			90E		
Time	Vol. Flow	Conversion	Time	Vol. Flow	Conversion	Time	Vol. Flow	Conversion
h	$\mu\text{L min}^{-1}$	%	h	$\mu\text{L min}^{-1}$	%	h	$\mu\text{L min}^{-1}$	%
2.3	130	Transient	2.4	130	Transient	2.5	95	Transient
3.7	135	65	4.3	132	55	6.1	99	62
6.1	130	56	6.2	130	53	14.3	98	55
8.4	130	50	8.4	131	52	24.7	97	52
13.4	130	46	10.8	127	43	35.9	96	47
24.7	76	Transient	14.6	95	Transient	46.6	97	45
28.1	74	44	25.1	98	40	55.5	98	42
30.9	78	40	29.5	97	39	75.4	66	Transient
48.5	75	33	32.2	95	38	81.2	61	41
52.7	75	35	38.0	53	Transient	98.5	66	44
55.4	76	32	49.0	54	47	120.7	43	Transient
72.8	76	25	54.1	53	49	147.5	43	43
75.6	74	28	74.8	54	41			
95.5	33	Transient	97.4	54	37			
100.9	32	40	118.3	54	33			
126.5	33	Transient	125.9	54	34			
144.3	32	26	140.0	54	29			
166.1	33	25	148.5	54	32			
			169.9	54	25			
			190.1	20	Transient			

Table S3. Initial rates and first-order deactivation rate constants for fructose dehydration at different space velocities and linear velocities, using catalyst E90

WHSV	Catalyst Mass	Initial Rate	Deactivation Rate Constant
h^{-1}	g	$\mu\text{mol min}^{-1} \text{g}^{-1}$	h^{-1}
0.48	0.173	13	0.011
0.48	0.346	23	0.015
4.0	0.050	48	0.053
4.0	0.100	43	0.081

^a In 1/4'' diameter reactor.

^b In 1/2'' diameter reactor.

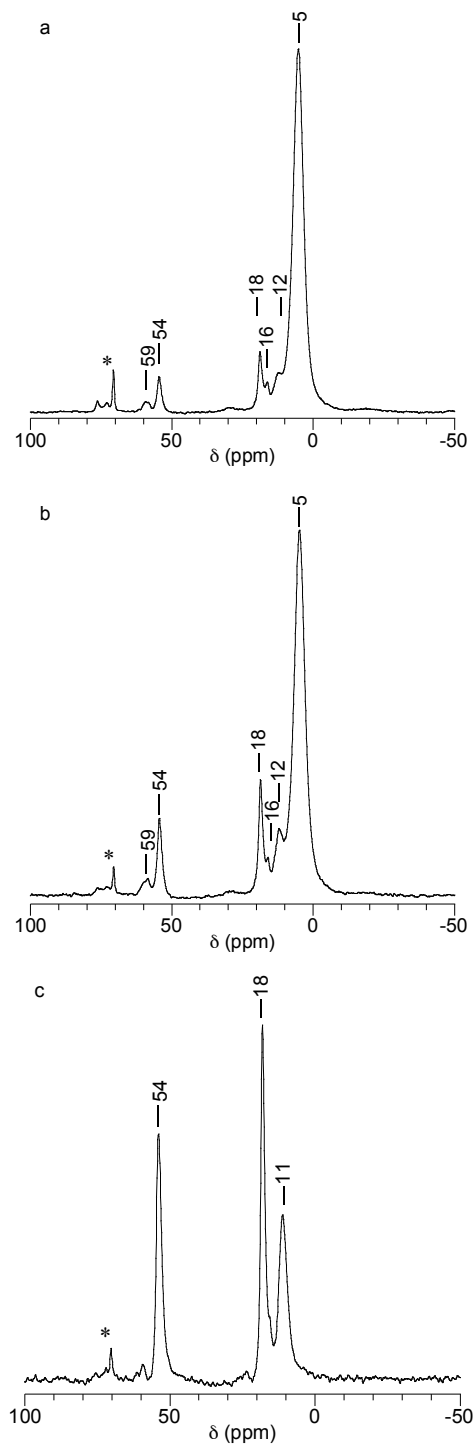


Figure S1. Solid-state ^{29}Si CP/MAS NMR spectra of various fresh pSO_3H -SBA-15-type catalysts: (a) E90; (b) E45; and (c) E0. Spinning rate 10 kHz. * indicates surfactant signals.

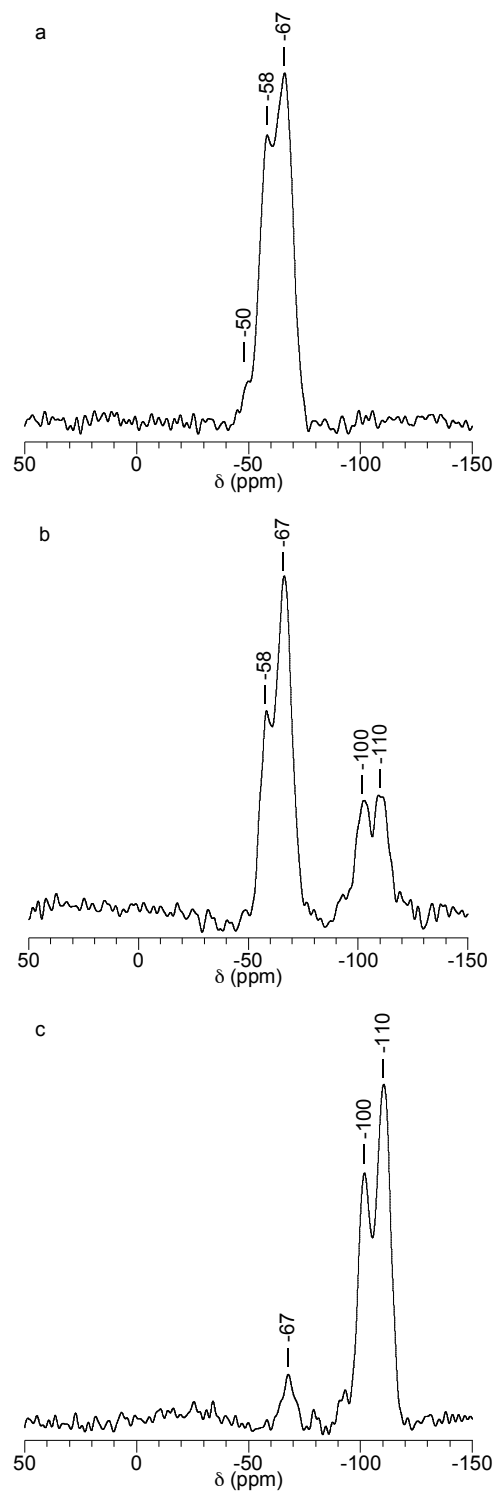


Figure S2. Solid-state ^{29}Si MAS NMR of pSO_3H -SBA-15 spectra of various fresh pSO_3H -SBA-15-type catalysts: (a) E90; (b) E45; and (c) E0. Spinning rate 10 kHz.

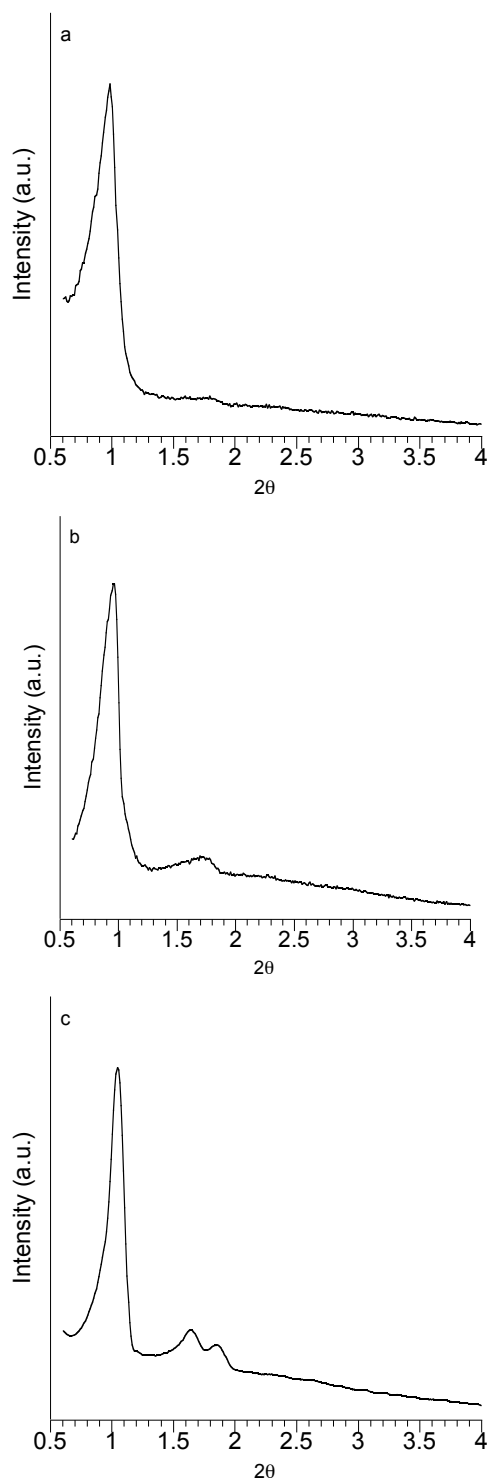


Figure S3. XRD reflection patterns for fresh $\text{pSO}_3\text{H-SBA-15}$ catalysts: (a) E90; (b) E45; and (c) E0.

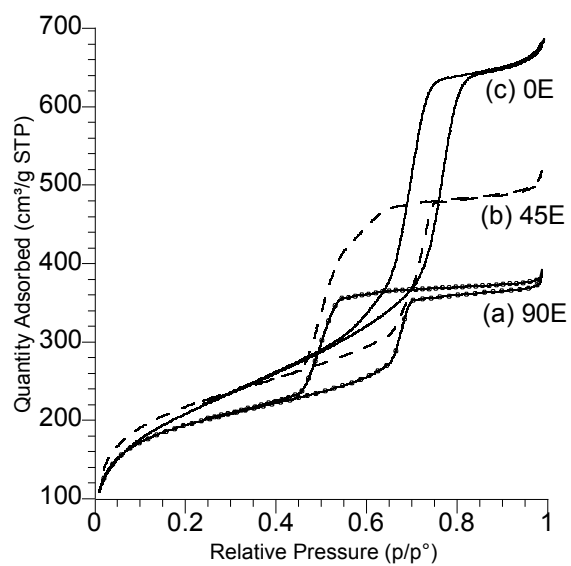


Figure S4. N₂ sorption isotherms for fresh pSO₃H-SBA-15 catalysts: (a) E90; (b) E45; and (c) E0.

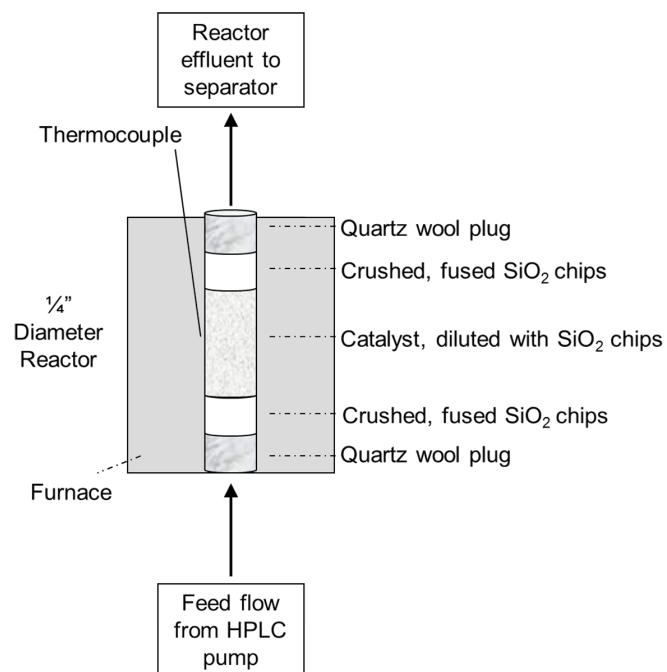


Figure S5. Schematic representation of alternate 1/4" reactor configuration. The design was implemented for times on-stream extending beyond 100 h.

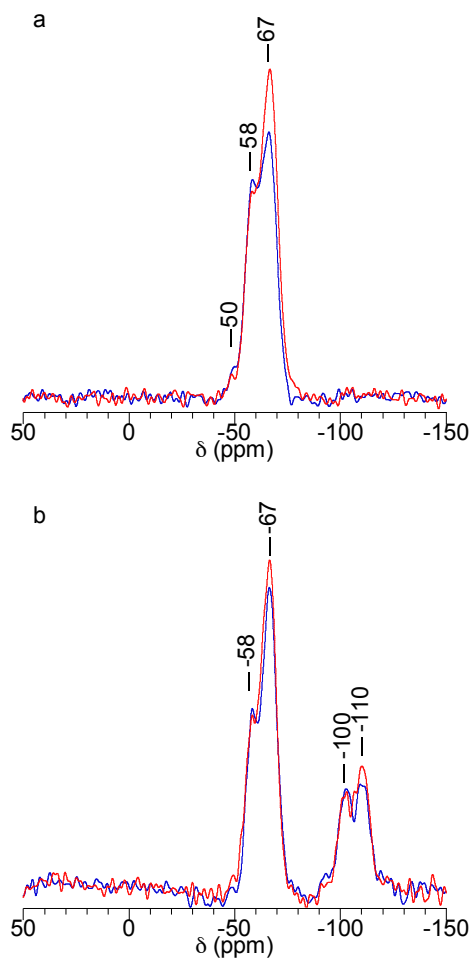


Figure S6. Solid-state ^{29}Si CP/MAS NMR spectra of various pSO_3H -SBA-15-type catalysts: (a) E90 and (b) E45; before (blue) and after (red) use on-stream at 403 K. E90, E45, and E0 were on-stream for 60, 51, and 55 h, respectively. Spinning rate 10 kHz.